

Critical probability distributions of the order parameter from the functional renormalization group

I. Balog,¹ A. Rançon,² and B. Delamotte³

¹*Institute of Physics, Bijenička cesta 46, HR-10001 Zagreb, Croatia*

²*Univ.Lille, CNRS, UMR 8523 – PhLAM – Laboratoire de Physique des Lasers Atomes et Molécules, F-59000 Lille, France*

³*Laboratoire de Physique Théorique de la Matière Condensée, UPMC, CNRS UMR 7600, Sorbonne Université, 4, place Jussieu, 75252 Paris Cedex 05, France*

(Dated: January 11, 2023)

We show that the functional renormalization group (FRG) allows for the calculation of the probability distribution function of the sum of strongly correlated random variables. On the example of the three-dimensional Ising model at criticality and using the simplest implementation of the FRG, we compute the probability distribution functions of the order parameter or equivalently its logarithm, called the rate functions in large deviations theory. We compute the entire family of universal scaling functions, obtained in the limit where the system size L and the correlation length of the infinite system ξ_∞ diverge, with the ratio $\zeta = L/\xi_\infty$ held fixed. It compares very accurately with numerical simulations.

In many different fields of research, mathematicians, physicists and even specialists of quantitative finance have paid considerable attention to the probability distribution of the sums of random variables. Here the Central Limit Theorem (CLT) plays a crucial role [1, 2]. It asserts that, given a large number N of independent identically distributed random variables $\hat{\sigma}_i$ with zero mean and finite variance, their sum $\hat{S} = \sum_i \hat{\sigma}_i$ has fluctuations of order \sqrt{N} , and the asymptotic probability distribution function (PDF) of \hat{S}/\sqrt{N} is a Gaussian law with finite variance. Most importantly, this result is independent of the probability law of the $\hat{\sigma}$'s, and the normal distribution plays the role of an attractor for the addition of an increasing number of random variables. The Gaussian distribution is therefore said to be stable and this is the most basic manifestation of what physicists call universality. The CLT has been generalized to the case where either the mean or the variance of the σ_i -law diverges: In this case, once it has been properly normalized, \hat{S} is distributed according to one of the celebrated Lévy-stable laws [3–5] that generalize the Gaussian law of the CLT.

The CLT can also be generalized to situations where the $\hat{\sigma}_i$ are correlated [2, 6]. If the correlation matrix G_{ij} decays sufficiently fast with a given “distance” r_{ij} between $\hat{\sigma}_i$ and $\hat{\sigma}_j$, such that $\sum_i G_{ij}$ is finite in the limit $N \rightarrow \infty$, the correlations are said to be weak. Then, the system behaves as if it were made of uncorrelated finite size clusters of $\hat{\sigma}_i$ and \hat{S} still has fluctuations of order \sqrt{N} . The CLT applies again, and the distribution of \hat{S}/\sqrt{N} is still Gaussian.

On the other hand, when $\sum_i G_{ij}$ diverges as $N \rightarrow \infty$, the fluctuations of \hat{S}/\sqrt{N} also diverge and the $\hat{\sigma}_i$ are said to be strongly correlated. Such situations are encountered in many different contexts, from critical systems, to out-of-equilibrium dynamics such as disease propagation, surface growth or turbulence. Our understanding of stable laws is much scarcer in this case. Nevertheless, it is reasonable to assume that properly normalized, $\hat{S}/f(N)$ should here again follow a stable law. Assum-

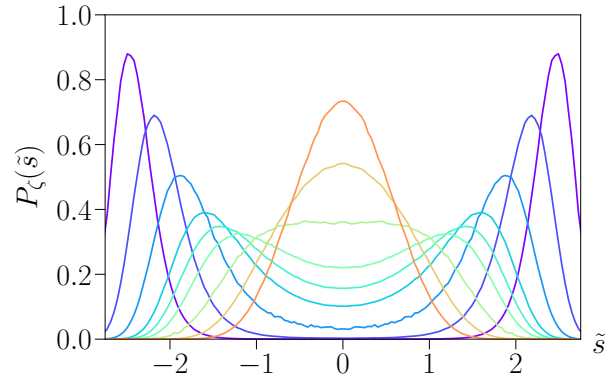


FIG. 1. Different critical PDFs of the 3d Ising model as functions of $\tilde{s} = L^{\frac{d-2+\eta}{2}} s$, obtained from Monte-Carlo simulations with periodic boundary conditions with $L = 128$ for various $\zeta = \text{sgn}(T - T_c)L/\xi_\infty(|T - T_c|)$, with $\zeta = -4$ to 4 by step of one (from bottom curve to top curve at the center).

ing universality, these laws, that are neither Gaussian nor Lévy, should depend only on a small number of parameters, such as the dimension of the system and its symmetries. These stable laws for strongly correlated variables have been observed experimentally or estimated numerically with relative ease [7–20]. On the theoretical side, a few exact results have been obtained in some specific models [21–29]. In generic models, the connections between CLT, stable laws and the fixed points of the Renormalization Group (RG) have been identified [30–32] since the early days of the Kadanoff-Wilson version of the RG [33]. However, it appears that these connections have remained at the conceptual level and have not been transformed into a set of techniques for calculating PDFs applicable to strongly correlated systems but in isolated cases with *ad hoc* methods [34–40]. Furthermore, the connection between RG and CLTs raises two paradoxes: 1) the PDF –being an observable– is RG-scheme independent, whereas fixed points are not; 2) as

discussed below, there is a family of critical rate functions, indexed by a real number ζ , but only one RG fixed point. We show here that the functional RG (FRG) in its modern version [41, 42] is the right framework to solve these paradoxes and compute quantitatively the PDF of strongly correlated random variables.

Let us briefly review the concepts fleshed out above in the context of the Ising model in the vicinity of its second order phase transition, on which we will focus from now on. The Hamiltonian of the ferromagnetic Ising model is $H = -J \sum_{\langle ij \rangle} \hat{\sigma}_i \hat{\sigma}_j$ with $J > 0$, $\hat{\sigma}_i = \pm 1$ and $\langle ij \rangle$ label nearest neighbor sites on a hypercubic d -dimensional lattice of linear size L with periodic boundary conditions. A second order phase transition occurs in the Ising model at some finite temperature T_c in $d > 1$ (we focus on the non-mean-field case $d < 4$). At fixed temperature $T \gtrsim T_c$ and for $r_{ij} \gg a$, a the lattice spacing, the correlation function of the spins behaves as $G_{ij} \sim r_{ij}^{-d+2-\eta} \exp(-r_{ij}/\xi_\infty)$ where $\eta \geq 0$ is the anomalous dimension of the spin field, and ξ_∞ the correlation length of the infinite system (at zero magnetic field), which diverges at the transition as $|t|^{-\nu}$, $t = T - T_c$. The condition of weak correlations is thus equivalent to the finiteness of ξ_∞ .

We are interested below in the PDF of the normalized total spin defined as $\hat{s} = L^{-d} \sum_i \hat{\sigma}_i$, the average of which is the magnetization $m = \langle \hat{s} \rangle$. The fluctuations of \hat{s} are measured by $\langle \hat{s}^2 \rangle$: $\langle \hat{s}^2 \rangle = L^{-d} \chi$, defining the magnetic susceptibility χ . For fixed $T \gtrsim T_c$, $\chi \sim \xi_\infty^{2-\eta}$ independent of L for $L \gg \xi_\infty$. This implies that the fluctuations of \hat{S}/\sqrt{N} are of order one: The system is weakly correlated. A precise calculation of the PDF is obtained from a saddle point approximation that becomes asymptotically exact when $L \rightarrow \infty$. As expected, it shows that the CLT holds and that the PDF becomes indeed Gaussian in this limit: $P(\hat{s} = s) \propto \exp(-\frac{L^d}{2\chi} s^2)$ for $T > T_c$ and $L \rightarrow \infty$ (at fixed $sL^{d/2}$) [43].

The argument above collapses at T_c and fixed L , where $\xi_\infty \gg L$, because χ scales with L as: $\chi \sim \int^L d^d r r^{-d+2-\eta} \sim L^{2-\eta}$ which diverges when $L \rightarrow \infty$. This implies that $\langle \hat{s}^2 \rangle \sim L^{-d+2-\eta}$ and that the fluctuations of \hat{S}/\sqrt{N} diverge as $L^{\frac{2-\eta}{2d}} = N^{\frac{2-\eta}{2d}}$. The spins are strongly correlated and the standard CLT does no longer hold: The saddle-point approximation fails and P has no reason to be a Gaussian anymore. However, the scaling of the fluctuations of \hat{s} suggest that P is a universal function of the scaling variable $\tilde{s} = s L^{\frac{d-2+\eta}{2}}$ [44].

It is rarely stressed that there is not only one PDF at criticality, but an infinity corresponding to the inequivalent ways to take the limit $L \rightarrow \infty$ and $T \rightarrow T_c^+$, i.e., $\xi_\infty \rightarrow \infty$, see Fig. 1 [45]. Indeed, choose any sequence $T_L > T_c$ converging to T_c , such that $\zeta = L/\xi_\infty(T_L)$ is constant. Then, for instance if $\xi_\infty(T_L) \ll L$ and from the discussion above, $\langle \hat{s}^2 \rangle \sim L^{-d} \chi \sim L^{-d+2-\eta} \zeta^{\eta-2}$. Once again, and even though $\xi_\infty(T_L)$ is finite at any L , the spins become more and more strongly correlated as $T_L \rightarrow T_c$. Therefore the PDF must be non-trivial for all values of ζ even in the limit $\zeta \gg 1$ (i.e. $\xi_\infty(T_L) \ll L$). In

this limit, we expect to recover some Gaussian-like features for typical values of s because the system looks for all $T_L > T_c$ as a collection of uncorrelated small blocks of spins of sizes $\xi_\infty(T_L)$. However, some non-gaussianity should remain in the tails of the PDF reminiscent of the strong correlations present at criticality where χ is diverging.

Assuming scaling, the PDF must depend on ξ_∞ and L only through the ratio ζ , which we parametrize as

$$P_\zeta(\hat{s} = s) \approx e^{-L^d I(s, \xi_\infty, L)} \approx e^{-I_\zeta(\tilde{s})}. \quad (1)$$

This relation defines the rate function $I(s, \xi_\infty, L)$, as it is known in large deviations theory (also known as the ‘‘constraint effective potential’’ in quantum field theory [46–48]), as well as its scaling function $I_\zeta(\tilde{s})$. Notice that we could define as well a family of universal critical PDFs when coming from the low temperature phase, $T \rightarrow T_c^-$. To tackle both cases at once, we define $\zeta = \text{sgn}(t)L/\xi_\infty(|t|)$. We show in Fig. 1 some of these PDFs obtained numerically (see below) in $d = 3$ with periodic boundary conditions.

These probabilistic arguments do not allow for computing $I_\zeta(\tilde{s})$. In the following we show that FRG yields a general formalism for such calculations. Being interested in universal PDFs, we replace the lattice Ising model by a \mathbb{Z}_2 -invariant field theory for which $\hat{s} = L^{-d} \int_{\mathbf{x}} \hat{\phi}(\mathbf{x})$ and thus:

$$P(\hat{s} = s) = \mathcal{N} \int \mathcal{D}\hat{\phi} \delta(s - \hat{s}) \exp(-\mathcal{H}[\hat{\phi}]), \quad (2)$$

with \mathcal{N} a normalization factor. Noting that the delta-function can be replaced by a infinitely peaked Gaussian, $\delta(z) \propto \exp(-M^2 z^2/2)$ with $M^2 \rightarrow \infty$, the PDF can be interpreted as the partition function \mathcal{Z}_M of a system with Hamiltonian $\mathcal{H}_M[\hat{\phi}] = \mathcal{H}[\hat{\phi}] + \frac{M^2}{2} \left(\int_{\mathbf{x}} (\hat{\phi}(\mathbf{x}) - s) \right)^2$, that is, $P(s) \propto \lim_{M \rightarrow \infty} \mathcal{Z}_M$. Remark that $M = 0$ corresponds to the standard partition function \mathcal{Z} of the model (at finite size L).

For a critical theory, the computation of \mathcal{Z}_M is plagued with the singularities induced by the long-distance/small-wavenumber fluctuations. The modern version of the FRG, tailored to deal with this difficulty [49–51], consists in freezing out these modes in the partition function while leaving unchanged the others and by gradually decreasing to zero the scale k that separates the low and high wavenumber modes: This generates the RG flow of partition functions or equivalently, of Hamiltonians.

A one-parameter family of models with partition functions $\mathcal{Z}_{M,k}[h]$ is thus built by changing the original Hamiltonian \mathcal{H}_M into $\mathcal{H}_M + \Delta\mathcal{H}_k - h \cdot \hat{\phi}$, where h is a magnetic field (or source) and the dot in $h \cdot \hat{\phi}$ implies an integral over space or momentum: $\mathcal{Z}_{M,k}[h] = \int \mathcal{D}\hat{\phi} \exp(-\mathcal{H}_M - \Delta\mathcal{H}_k + h \cdot \hat{\phi})$. Here, $\Delta\mathcal{H}_k$ is the term designed to effectively freeze the low wavenumber fluctuations $\hat{\phi}(|\mathbf{q}| < k)$ while leaving unchanged the high wavenumber modes $\hat{\phi}(|\mathbf{q}| > k)$. It is chosen quadratic:

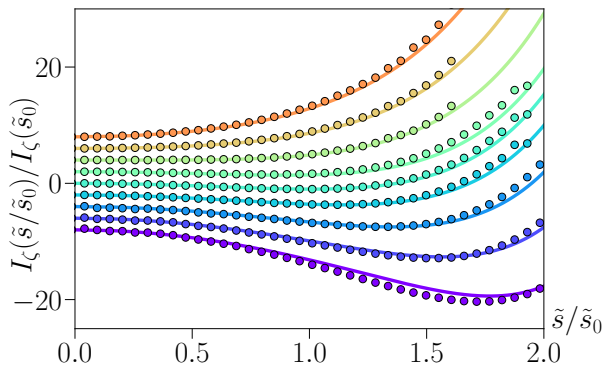


FIG. 2. Normalized rate functions $I_\zeta(\tilde{s})$ of the 3d Ising model obtained from FRG (full line) and MC simulations (symbols) performed on the cubic lattice with periodic boundary conditions for $\zeta = -4$ to 4 (from bottom to top, same color code as in Fig. 1). The normalization point \tilde{s}_0 is the position of the minimum of $I_{\zeta=0}$. The rate functions have been shifted for better visibility.

$\Delta\mathcal{H}_k = 1/2 \hat{\phi} \cdot R_k \cdot \hat{\phi}$ with $R_k(\mathbf{x}, \mathbf{y})$ such that (i) when $k \sim a^{-1}$, $R_{k \sim a^{-1}}(|\mathbf{q}|)$ is very large for all $|\mathbf{q}|$ which implies that all fluctuations are frozen; and (ii) $R_{k=0}(|\mathbf{q}|) \equiv 0$ so that all fluctuations are integrated over and $\mathcal{Z}_{M,k=0}[h] = \mathcal{Z}_M[h]$. Varying the scale k between a^{-1} and 0 induces the RG flow of $\mathcal{Z}_{M,k}[h]$, in which fluctuations of wavenumbers $|\mathbf{q}| > k$ are progressively integrated over.

Actual calculations of $\mathcal{Z}_{M,k}[h]$ require to perform approximations that are known to be controlled only when working with the (slightly modified) Legendre transform of $\log \mathcal{Z}_{M,k}[h]$ with respect to h , $\Gamma_{M,k}[\phi]$ [52–54], defined as

$$\Gamma_{M,k}[\phi] = -\ln \mathcal{Z}_{M,k}[h] + h \cdot \phi - \frac{1}{2} \phi \cdot R_k \cdot \phi - \frac{M^2}{2} \{\phi - s\}^2, \quad (3)$$

where $\{\phi - s\}^2 \equiv (\int_{\mathbf{x}} (\phi(\mathbf{x}) - s))^2$ and $\phi(\mathbf{x}) = \langle \hat{\phi}(\mathbf{x}) \rangle = \frac{\delta \mathcal{Z}_{M,k}}{\delta h(\mathbf{x})}$. It can also be defined as (see Suppl. Mat. [55])

$$e^{-\Gamma_{M,k}[\phi]} = \int \mathcal{D}\hat{\phi} e^{-\mathcal{H}[\hat{\phi}] - \frac{1}{2}(\hat{\phi} - \phi) \cdot R_{M,k} \cdot (\hat{\phi} - \phi) + \frac{\delta \Gamma_{M,k}}{\delta \phi} \cdot (\hat{\phi} - \phi)}, \quad (4)$$

where $R_{M,k}(\mathbf{x}, \mathbf{y}) = R_k(\mathbf{x}, \mathbf{y}) + M^2$, or in momentum space $R_{M,k}(\mathbf{q}) = R_k(\mathbf{q}) + M^2 \delta_{\mathbf{q},0}$, with $\mathbf{q} = \frac{2\pi}{L} \mathbf{n}$ and $\mathbf{n} \in \mathbb{Z}^d$. Eq. (4) has the advantage of explicitly showing that $\Gamma_{M,k}$ does not depend on s . Up to the replacement of R_k by $R_{M,k}$, $\Gamma_{M,k}$ is formally identical to the usual scale-dependent effective action Γ_k introduced in FRG [42], and indeed, $\Gamma_k[\phi] = \Gamma_{M=0,k}[\phi]$. The exact RG equation satisfied by $\Gamma_{M,k}[\phi]$ is the usual Wetterich equation in the presence of the regulator $R_{M,k}$:

$$\partial_k \Gamma_{M,k}[\phi] = \frac{1}{2} \int_{\mathbf{x}, \mathbf{y}} \partial_k R_{M,k}(\mathbf{x}, \mathbf{y}) \left(\Gamma_{M,k}^{(2)} + R_{M,k} \right)^{-1}(\mathbf{x}, \mathbf{y}), \quad (5)$$

where $\Gamma_{M,k}^{(2)} = \Gamma_{M,k}^{(2)}[\mathbf{x}, \mathbf{y}; \phi] = \frac{\delta^2 \Gamma_{M,k}}{\delta \phi(\mathbf{x}) \delta \phi(\mathbf{y})}$.

Defining $\tilde{\Gamma}_k[\phi] = \lim_{M \rightarrow \infty} \Gamma_{M,k}[\phi]$, the additional k -independent term $M^2 \delta_{\mathbf{q},0}$ completely freezes the zero-momentum mode $\int_{\mathbf{x}} \hat{\phi}(\mathbf{x})$ in $\tilde{\Gamma}_k[\phi]$, and we show in [55] that when evaluated in constant field $\phi(\mathbf{x}) = s$, $L^{-d} \tilde{\Gamma}_k[s] = I_k(s)$ is a scale dependent rate function such that $P(s) \propto \lim_{k \rightarrow 0} \exp(-L^d I_k(s))$. [In contrast, when evaluated in a constant field $\phi(\mathbf{x}) = m$, the effective action $\Gamma_k[\phi = m]$ is $L^d U_k(m)$ where $U_k(m)$ is the k -dependent effective potential that becomes the true effective potential at $k = 0$. In particular, $\Gamma[\phi] = \Gamma_{k=0}[\phi]$ being the Legendre transform of $\ln \mathcal{Z}[h]$, the effective potential $U(m) = U_{k=0}(m)$ is a convex function of m [42]. Note that both Γ and I are RG-scheme independent by construction.] Our aim in the following is to compute $\tilde{\Gamma}_k[\phi = s]$ and to evaluate it at $k = 0$. For this purpose, we now study the flow of $\tilde{\Gamma}_k$ comparing it with the better known flow of Γ_k .

For $\zeta \ll 1$ and $a^{-1} \gg k \gg 1/L \gg 1/\xi_\infty$, the regulator R_k effectively freezes the zero-momentum mode in Γ_k , which makes its flow identical to that of $\tilde{\Gamma}_k$, up to corrections of order $(kL)^{-d}$. In this range of k , the system is self-similar because both a and L play no role in the flows. It follows that both U_k and I_k obey a scaling form $I_k(\phi) \simeq U_k(\phi) = k^d \tilde{U}^*(\phi k^{-(d-2+\eta)/2})$, where \tilde{U}^* is k -independent, that is, it is the dimensionless fixed point potential of the RG flow of Γ_k [42]. It is a non-convex function that has the typical double well form, see below.

When k becomes of order $2\pi/L$, the flows of U_k and I_k start to differ significantly. On the one hand, the flow of U_k becomes essentially that of a zero-dimensional system (corresponding to the fluctuations of the zero-momentum mode only), and $\lim_{k \rightarrow 0} U_k(m)$ becomes convex with a curvature at small m given by $\chi^{-1} \propto L^{-2+\eta}$. On the other hand, the flow of $I_k(s)$ stops typically for $k \lesssim 2\pi/L$ because in this quantity the zero-momentum mode is frozen by the $M \rightarrow \infty$ term. In particular, this allows for a non-convex shape of $I(s) = I_{k=0}(s)$ and $L^d I(s)$ is found to naturally be a function of $\tilde{s} = sL^{\frac{d-2+\eta}{2}}$.

The above picture is modified when $\zeta \gg 1$ ($T > T_c$, $L \gg \xi_\infty$), because the system size can no longer play any significant role when $\xi_\infty \ll L$. In particular, the flows of U_k and I_k rapidly stop for $k \lesssim 1/\xi_\infty$ and it makes no difference whether the zero mode is completely frozen or not. Approaching criticality from the disordered phase, we therefore find that $I_{k=0}(s) \simeq U_{k=0}(m = s)$. These functions are convex with positive curvature $\chi^{-1} \propto \xi_\infty^{-2+\eta}$ at $s = 0$. Working at fixed ζ , we thus have $L^d I_{k=0}(s) \propto \zeta^{2-\eta} L^{d-2+\eta} s^2$ at small s . The PDF is therefore Gaussian at small s as in the CLT, which is expected because the system looks like a collection of uncorrelated clusters of spins of extension ξ_∞ . However, since the susceptibility diverges at $T = T_c$ as $\xi_\infty^{-2+\eta}$, the fluctuations are anomalously large compared with the usual CLT because they are of order $L^{-\frac{d-2+\eta}{2}}$ instead of the standard $L^{-d/2}$. Varying ζ then generates a smooth family of rate functions, the shapes of which depend on the competition between L and ξ_∞ in the flow. Furthermore, $I_\zeta(\tilde{s})$

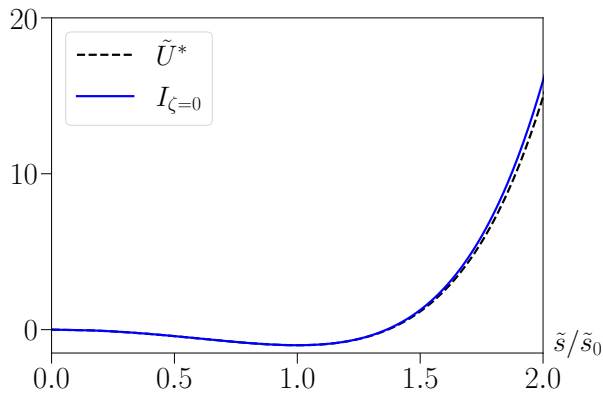


FIG. 3. Scaling rate function at $\zeta = 0$ obtained from FRG (blue) as a function of \tilde{s} , and fixed point potential obtained with the same regulator as function of $\phi = \tilde{s}$. Both have been normalized such that their minimum is -1 at 1 . The difference is only visible in the tail.

behaves as $\tilde{s}^{\frac{2d}{d-2+\eta}}$ at large \tilde{s} , a behavior inherited from \tilde{U}^* [55].

To compute in practice the rate function and find its specific shape depending on ζ , it is necessary to solve the flow equation Eq. (5). This cannot be done exactly, and it is necessary to perform approximations. Here, we focus on the simplest of such approximations which nevertheless allows for a functional calculation of the rate function, the so-called Local Potential Approximation (LPA). It amounts to using the Ansatz $\tilde{\Gamma}_k[\phi] = \int_{\mathbf{x}} (\frac{1}{2}(\partial\phi)^2 + I_k(\phi(\mathbf{x})))$, and projecting the flow equation onto this Ansatz. The corresponding LPA flow equation is then closed for the scale-dependent rate function and reads

$$\partial_k I_k(s) = \frac{1}{2L^d} \sum_{\mathbf{q} \neq 0} \frac{\partial_k R_k(\mathbf{q})}{\mathbf{q}^2 + R_k(\mathbf{q}) + I_k''(s)}, \quad (6)$$

and we use the “exponential regulator” $R_k(\mathbf{q}) = \alpha k^2 e^{-\mathbf{q}^2/k^2}$ with $\alpha = 4.65$ [55]. Note that at LPA the anomalous dimension vanishes, $\eta = 0$, but since $\eta \ll 1$ for the three-dimensional Ising model, we expect the approximation to correctly capture the shape of the rate function. The scaling functions $I_\zeta(\tilde{s}) = I_{\zeta, k=0}(\tilde{s})$ obtained from integrating the LPA flow, Eq. (6), are shown as solid lines in Fig. 2 for various ζ , see [55]. We have verified that the resulting rate functions obey the expected scaling, are functions of \tilde{s} and ζ only, and only very weakly depend on the regulator function R_k [55].

In the same figure, we compare our FRG results to the rate functions obtained from Monte-Carlo (MC) simulations on the cubic lattice with periodic boundary conditions, using a Wolff algorithm [60] with histogram reweighting [61], also used to generate Fig. 1, see [55]. Since lattice and field theory calculations use different units, it requires rescalings of the x -axis (magnitude of the total spin s) and y -axis (associated to the microscopic length scales, since $I(s)$ is a density) in the plot of

$I(s)$, Fig. 2. Importantly, these model-dependent lengths are independent of ζ , and should be determined from only one value of ζ (we use $\zeta = 0$). We find that to compare the rate function obtained from MC for a given ζ_{MC} to that obtained from LPA at ζ_{LPA} necessitates a rescaling of ζ_{LPA} , with $\zeta_{\text{MC}} \simeq 0.9 \zeta_{\text{LPA}}$ [55]. We attribute this to errors in the computation of ξ_∞ induced by LPA. With this small caveat, we find a very good agreement between simulations and FRG on the whole range of $\zeta \in [-4, 4]$. Note that the rate functions become strictly convex for $\zeta \gtrsim 2.2$.

It is interesting to note that $I_{\zeta=0}$ is very similar to the fixed point potential, when properly normalized, see Fig. 3. This could explain why the fixed point of the RG has long been thought to describe the critical PDFs [34, 38, 40]. However, this cannot be true exactly because the dependence of the fixed point effective potential \tilde{U}^* on the choice of regulator R_k cannot be normalized out. This can be shown explicitly in the large N limit of the critical $O(N)$ model [62]. Reciprocally, our work confirms that RG is deeply related to probability theory since computing a fixed point is actually almost synonymous to computing the $I_{\zeta=0}$ but for the zero-mode which is excluded in the rate function. This elucidates the long-standing paradoxes arising from the confusion between the fixed point potential \tilde{U}^* and $I_{\zeta=0}$ which, although very closely related, are conceptually different.

Our work raises many questions and paves the way to many applications that we want to briefly review below. For instance, the method can be generalized to all pure statistical systems at thermal equilibrium, with probably very good results at least when the LPA is accurate, that is, when η is small. The generalization to disordered and/or out of equilibrium systems, where very little is known about the computation of critical PDFs, certainly requires to adapt the formalism. This should be feasible since FRG already yields fairly accurate results for such problems like the random field $O(N)$ models [63–65], reaction-diffusion models [66, 67] and the Kardar-Parisi-Zhang equation [68–71] to mention just a few [42]. Also, the coexistence region in the low-temperature phase is highly non-trivial, scaling as a surface term, and necessitates to go beyond LPA, which does not capture domain walls. This could explain why our results do not agree as well with MC simulations for large and negative ζ . However, the LPA can be systematically improved via a derivative expansion or the Blaizot-Mendez-Wschebor approximation scheme [72, 73]. The study of the convergence along the lines of [53, 54] for the rate function is left for future work.

ACKNOWLEDGMENTS

We thank O. Bénichou, N. Dupuis, G. Tarjus and N. Wschebor for discussions and feedbacks. BD thanks F. Benitez, M. Tissier and Z. Rácz for many discussions in an early stage of this work. AR also thanks G. Verley for

discussions on this and related subjects. IB acknowledges the support of the the QuantiXLie Centre of Excellence, a project cofinanced by the Croatian Government and European Union through the European Regional Development Fund - the Competitiveness and Cohesion Oper-

ational Programme (Grant KK.01.1.1.01.0004). BD acknowledges the support from the French ANR through the project NeqFluids (grant ANR-18-CE92-0019). AR is supported by the Research Grants QRITiC I-SITE ULNE/ ANR-16-IDEX-0004 ULNE.

-
- [1] W. Feller, *An introduction to Probability Theory, Vols 1 and 2* (Wiley, New York, 1971).
- [2] R. Botet and M. Płoszajczak, *Universal Fluctuations: The Phenomenology of Hadronic Matter* (2002).
- [3] P. Lévy, *Théorie de l'addition des variables aléatoires*, Collection des monographies des probabilités (Gauthier-Villars, 1954).
- [4] B. V. Gnedenko and A. N. Kolmogorov, *Limit distributions for sums of independent random variables* (Cambridge, Mass: Addison-Wesley Pub. Co., 1954).
- [5] O. C. Ibe, in *Markov Processes for Stochastic Modeling (Second Edition)*, edited by O. C. Ibe (Elsevier, Oxford, 2013) second edition ed., pp. 329–347.
- [6] J. Dedecker, P. Doukhan, G. Lang, L. R. J. Rafael, S. Louhichi, and C. Prieur, *Weak Dependence: With Examples and Applications* (Springer New York, 2007).
- [7] K. Binder, Phys. Rev. Lett. **47**, 693 (1981).
- [8] K. Binder, Zeitschrift für Physik B Condensed Matter **43**, 119 (1981).
- [9] A. D. Bruce and N. B. Wilding, Phys. Rev. Lett. **68**, 193 (1992).
- [10] D. Nicolaides and A. D. Bruce, Journal of Physics A: Mathematical and General **21**, 233 (1988).
- [11] M. M. Tsy-pin, Phys. Rev. Lett. **73**, 2015 (1994).
- [12] C. Alexandrou, A. Boriçi, A. Feo, P. de Forcrand, A. Galli, F. Jergerlehner, and T. Takahashi, Phys. Rev. D **60**, 034504 (1999).
- [13] M. M. Tsy-pin and H. W. J. Blöte, Phys. Rev. E **62**, 73 (2000).
- [14] S. T. Bramwell, P. C. W. Holdsworth, and J. F. Pinton, Nature (London) **396**, 552 (1998).
- [15] S. T. Bramwell, K. Christensen, J. Y. Fortin, P. C. W. Holdsworth, H. J. Jensen, S. Lise, J. M. López, M. Nicodemi, J. F. Pinton, and M. Sellitto, Phys. Rev. Lett. **84**, 3744 (2000).
- [16] B. Portelli and P. C. W. Holdsworth, Journal of Physics A Mathematical General **35**, 1231 (2002).
- [17] K. A. Takeuchi and M. Sano, Phys. Rev. Lett. **104**, 230601 (2010).
- [18] P. H. L. Martins, Phys. Rev. E **85**, 041110 (2012).
- [19] A. Malakis, N. G. Fytas, and G. Gülpinar, Phys. Rev. E **89**, 042103 (2014).
- [20] J. Xu, A. M. Ferrenberg, and D. P. Landau, Phys. Rev. E **101**, 023315 (2020).
- [21] F. J. Dyson, Communications in Mathematical Physics **12**, 91 (1969).
- [22] P. M. Bleher and J. G. Sinai, Communications in Mathematical Physics **33**, 23 (1973).
- [23] P. Collet and J.-P. Eckmann, *A Renormalization Group Analysis of the Hierarchical Model in Statistical Mechanics* (Springer Berlin, Heidelberg, 1978).
- [24] P. M. Bleher and P. Major, The Annals of Probability **15**, 431 (1987).
- [25] J. Brankov and D. Danchev, Physica A: Statistical Mechanics and its Applications **158**, 842 (1989).
- [26] T. Antal, M. Droz, and Z. Rácz, Journal of Physics A: Mathematical and General **37**, 1465 (2004).
- [27] T. Sasamoto and H. Spohn, Phys. Rev. Lett. **104**, 230602 (2010).
- [28] B. M. McCoy and T. T. Wu, *The Two-Dimensional Ising Model* (Harvard University Press, 2013).
- [29] F. Camia, C. Garban, and C. M. Newman, Annales de l'Institut Henri Poincaré, Probabilités et Statistiques **52**, 146 (2016).
- [30] G. Jona-Lasinio, Il Nuovo Cimento B (1971-1996) **26**, 99 (1975).
- [31] G. Gallavotti and A. Martin-Löf, Il Nuovo Cimento B (1971-1996) **25**, 425 (1975).
- [32] M. Cassandro and G. Jona-Lasinio, Advances in Physics **27**, 913 (1978).
- [33] K. G. Wilson and J. B. Kogut, Phys. Rept. **12**, 75 (1974).
- [34] A. D. Bruce, T. Schneider, and E. Stoll, Phys. Rev. Lett. **43**, 1284 (1979).
- [35] E. Eisenriegler and R. Tomaschitz, Phys. Rev. B **35**, 4876 (1987).
- [36] R. Hilfer, International Journal of Modern Physics B **07**, 4371 (1993).
- [37] R. Hilfer and N. B. Wilding, Journal of Physics A: Mathematical and General **28**, L281 (1995).
- [38] A. Esser, V. Dohm, and X. Chen, Physica A: Statistical Mechanics and its Applications **222**, 355 (1995).
- [39] A. D. Bruce, Phys. Rev. E **55**, 2315 (1997).
- [40] J. Rudnick, W. Lay, and D. Jasnow, Phys. Rev. E **58**, 2902 (1998).
- [41] J. Berges, N. Tetradis, and C. Wetterich, Physics Reports **363**, 223 (2002).
- [42] N. Dupuis, L. Canet, A. Eichhorn, W. Metzner, J. Pawłowski, M. Tissier, and N. Wschebor, Physics Reports **910**, 1 (2021).
- [43] J. Zinn-Justin, *Phase transitions and renormalization group* (2007).
- [44] J.-P. Bouchaud and A. Georges, Physics Reports **195**, 127 (1990).
- [45] The shapes of the family of PDFs also depend crucially on the boundary conditions [8]. Here we focus on periodic boundary conditions only.
- [46] R. Fukuda and E. Kyriakopoulos, Nuclear Physics B **85**, 354 (1975).
- [47] L. O'Raifeartaigh, A. Wipf, and H. Yoneyama, Nuclear Physics B **271**, 653 (1986).
- [48] M. Göckeler and H. Leutwyler, Nuclear Physics B **350**, 228 (1991).
- [49] C. Wetterich, Nuclear Physics B **352**, 529 (1991).
- [50] C. Wetterich, Physics Letters B **301**, 90 (1993).
- [51] C. Wetterich, Zeitschrift für Physik C **60**, 461 (1993).
- [52] L. Canet, B. Delamotte, D. Mouhanna, and J. Vidal, Phys. Rev. B **68**, 064421 (2003).

- [53] I. Balog, H. Chaté, B. Delamotte, M. Marohnić, and N. Wschebor, Physical Review Letters **123**, 240604 (2019).
- [54] G. De Polsi, I. Balog, M. Tissier, and N. Wschebor, Phys. Rev. E **101**, 042113 (2020).
- [55] See Supplementary Material the derivation of $\Gamma_{M,k}$, its flow equation, and the numerical solution of the flow; details on the Monte-Carlo simulations. It also includes Refs. [56-59].
- [56] L. Fister and J. M. Pawłowski, Phys. Rev. D **92**, 076009 (2015).
- [57] P. Lundow and I. Campbell, Physica A **511**, 40 (2018).
- [58] A. M. Ferrenberg, J. Xu, and D. P. Landau, Phys. Rev. E **97**, 043301 (2018).
- [59] F. Kos, D. Poland, D. Simmons-Duffin, and A. Vichi, Journal of High Energy Physics **2016**, 36 (2016).
- [60] U. Wolff, Phys. Rev. Lett. **62**, 361 (1989).
- [61] A. M. Ferrenberg and R. H. Swendsen, Phys. Rev. Lett. **61**, 2635 (1988).
- [62] I. Balog, A. Raçon and B. Delamotte, to be published.
- [63] G. Tarjus and M. Tissier, Phys. Rev. Lett. **93**, 267008 (2004).
- [64] M. Tissier and G. Tarjus, Phys. Rev. Lett. **107**, 041601 (2011).
- [65] M. Tissier and G. Tarjus, Phys. Rev. B **85**, 104202 (2012).
- [66] L. Canet, B. Delamotte, O. Deloubrière, and N. Wschebor, Phys. Rev. Lett. **92**, 195703 (2004).
- [67] L. Canet, H. Chaté, B. Delamotte, I. Dornic, and M. A. Muñoz, Phys. Rev. Lett. **95**, 100601 (2005).
- [68] L. Canet, H. Chaté, B. Delamotte, and N. Wschebor, Phys. Rev. Lett. **104**, 150601 (2010).
- [69] L. Canet, H. Chaté, B. Delamotte, and N. Wschebor, Phys. Rev. E **84**, 061128 (2011).
- [70] T. Kloss, L. Canet, B. Delamotte, and N. Wschebor, Phys. Rev. E **89**, 022108 (2014).
- [71] L. Canet, B. Delamotte, and N. Wschebor, Phys. Rev. E **93**, 063101 (2016).
- [72] J.-P. Blaizot, R. Méndez-Galain, and N. Wschebor, Physics Letters B **632** (2006).
- [73] F. Benitez, J.-P. Blaizot, H. Chaté, B. Delamotte, R. Méndez-Galain, and N. Wschebor, Phys. Rev. E **80**, 030103(R) (2009).

SUPPLEMENTAL MATERIALS

I. DEFINITION OF THE EFFECTIVE ACTIONS $\Gamma_{M,k}$

We start from the M -dependent partition functions in presence of a regulator R_k and a source h as defined in the main text:

$$\mathcal{Z}_{M,k}[h] = \int \mathcal{D}\hat{\phi} e^{-\mathcal{H}_M[\hat{\phi}] + h \cdot \hat{\phi} - \frac{1}{2} \hat{\phi} \cdot R_k \cdot \hat{\phi}} \quad (7)$$

where $\mathcal{H}_M[\hat{\phi}] = \mathcal{H}(\hat{\phi}) + \frac{M^2}{2} [\int_{\mathbf{x}} (\hat{\phi}(\mathbf{x}) - s)]^2$.

Using $\phi(\mathbf{x}) = \frac{\delta \mathcal{Z}_{M,k}}{\delta h(\mathbf{x})}$, we define the modified Legendre

transform

$$\Gamma_{M,k}[\phi] = -\ln \mathcal{Z}_{M,k}[h] + h \cdot \phi - \frac{1}{2} \phi \cdot R_k \cdot \phi - \frac{M^2}{2} \left[\int_{\mathbf{x}} (\phi(\mathbf{x}) - s) \right]^2 \quad (8)$$

Note that

$$\frac{\delta \Gamma_{M,k}}{\delta \phi(\mathbf{x})} = h(\mathbf{x}) - \int_{\mathbf{y}} R_k(\mathbf{x}, \mathbf{y}) \phi(\mathbf{y}) - M^2 \int_{\mathbf{y}} (\phi(\mathbf{y}) - s). \quad (9)$$

which allows us to write

$$e^{-\Gamma_{M,k}[\phi]} = \int \mathcal{D}\hat{\phi} e^{-\mathcal{H}(\hat{\phi}) + \frac{\delta \Gamma_{M,k}}{\delta \phi} \cdot (\hat{\phi} - \phi) - \frac{1}{2} (\hat{\phi} - \phi) \cdot R_k \cdot (\hat{\phi} - \phi)} \times e^{-\frac{M^2}{2} [\int_{\mathbf{x}} (\hat{\phi}(\mathbf{x}) - \phi(\mathbf{x}))]^2}. \quad (10)$$

Defining $R_{M,k}(\mathbf{x}, \mathbf{y}) = R_k(\mathbf{x}, \mathbf{y}) + M^2$, this equation can be rewritten as:

$$e^{-\Gamma_{M,k}[\phi]} = \int \mathcal{D}\hat{\phi} e^{-\mathcal{H}(\hat{\phi}) + \frac{\delta \Gamma_{M,k}}{\delta \phi} \cdot (\hat{\phi} - \phi) - \frac{1}{2} (\hat{\phi} - \phi) \cdot R_{M,k} \cdot (\hat{\phi} - \phi)}, \quad (11)$$

and therefore $\Gamma_{M,k}[\phi]$ can be interpreted as the (modified) Gibbs free energy of a system of Hamiltonian \mathcal{H} instead of \mathcal{H}_M regularized by $R_{M,k}$ instead of R_k .

Note that although it is not explicit from its definition, Eq.(8), $\Gamma_{M,k}[\phi]$ is independent of s as can be checked from Eq.(11) or by deriving Eq. (8) with respect to s .

When evaluated in a constant field $\phi(\mathbf{x}) = s$ and at $k = 0$,

$$\left. \frac{\delta \Gamma_{M,k=0}}{\delta \phi(\mathbf{x})} \right|_{\phi(\mathbf{x})=s} = h \quad (12)$$

is a constant, by translation invariance, such that $\langle \hat{\phi}(\mathbf{x}) \rangle = s$. Thus,

$$e^{-\Gamma_{M,k=0}[\phi(\mathbf{x})=s]} = \int \mathcal{D}\hat{\phi} e^{-\mathcal{H}(\hat{\phi}) - \frac{M^2}{2} [\int_{\mathbf{x}} (\hat{\phi} - s)]^2 + h \int_{\mathbf{x}} (\hat{\phi} - s)}, \quad (13)$$

and therefore

$$\lim_{M \rightarrow \infty} e^{-\Gamma_{M,k=0}[\phi(\mathbf{x})=s]} \propto \int \mathcal{D}\hat{\phi} \delta \left(s - L^{-d} \int_{\mathbf{x}} \hat{\phi} \right) e^{-\mathcal{H}(\hat{\phi})} \propto P(s). \quad (14)$$

This directly proves that $\lim_{M \rightarrow \infty} \Gamma_{M,k=0}[\phi(\mathbf{x}) = s] = L^d I(s)$. For finite k , it is convenient to define $\check{\Gamma}_k[\phi] = \lim_{M \rightarrow \infty} \Gamma_{M,k}[\phi]$, and we interpret $L^{-d} \check{\Gamma}_k[\phi(\mathbf{x}) = s] = I_k(s)$ as a scale-dependent rate function.

The similar construction at $M = 0$ gives rise to the standard scale-dependent effective action $\Gamma_k[\phi]$ introduced in the FRG [42].

Note that at $k = 0$, $\Gamma[\phi] = \Gamma_{k=0}[\phi]$ is the (true) Legendre transform of $\ln \mathcal{Z}_{M=0}[h]$ (since the regulator R_k identically vanishes in this limit) and is therefore a convex functional. On the contrary, $\check{\Gamma}[\phi] = \check{\Gamma}_{k=0}[\phi]$ is not a true Legendre transform even in this limit, due to the M term in Eq. (8), and can therefore be non-convex.

II. FLOW EQUATIONS OF THE EFFECTIVE ACTIONS $\Gamma_{M,k}$ AND LOCAL POTENTIAL APPROXIMATION

The initial condition of the flow corresponds to $k = \Lambda$, for which $\lim_{k \rightarrow \Lambda} R_k(\mathbf{q}) \rightarrow \infty$. A saddle-point analysis gives

$$\lim_{k \rightarrow \Lambda} \mathcal{Z}_{M,k}[h] \simeq e^{-\mathcal{H}_M[\phi] + h \cdot \phi - \frac{1}{2} \phi \cdot R_\Lambda \cdot \phi}, \quad (15)$$

with $\phi[h]$ such that

$$\frac{\delta \mathcal{H}_M}{\delta \phi(\mathbf{x})} - h(\mathbf{x}) + \int_{\mathbf{y}} R_\Lambda(\mathbf{x}, \mathbf{y}) \phi(\mathbf{y}) = 0. \quad (16)$$

Performing the Legendre transform and using Eq. (8), we obtain

$$\lim_{k \rightarrow \infty} \Gamma_{M,k}[\phi] = \mathcal{H}[\phi]. \quad (17)$$

The effective actions $\Gamma_{M,k}$ obey the exact flow equation

$$\partial_k \Gamma_{M,k}[\phi] = \frac{1}{2} \int_{\mathbf{x}, \mathbf{y}} \partial_k R_{M,k}(\mathbf{x}, \mathbf{y}) \left(\Gamma_{M,k}^{(2)} + R_{M,k} \right)^{-1}(\mathbf{x}, \mathbf{y}), \quad (18)$$

where

$$\Gamma_{M,k}^{(2)} = \Gamma_{M,k}^{(2)}[\mathbf{x}, \mathbf{y}; \phi] = \frac{\delta^2 \Gamma_{M,k}}{\delta \phi(\mathbf{x}) \delta \phi(\mathbf{y})}, \quad (19)$$

as can be derived by using the standard properties of Legendre transforms [42].

The Local Potential Approximation corresponds to the approximation

$$\Gamma_{M,k}[\phi] = \int_{\mathbf{x}} \left(\frac{(\partial \phi)^2}{2} + U_{M,k}(\phi(\mathbf{x})) \right), \quad (20)$$

from which follows the inverse propagator in momentum space and in constant field ϕ

$$\Gamma_{M,k}^{(2)}(\mathbf{q}, \phi) = \mathbf{q}^2 + U''_{M,k}(\phi). \quad (21)$$

In this approximation, the only flowing quantity is $U_{M,k}$, and its flow equation reads

$$\partial_k U_{M,k}(\phi) = \frac{1}{2L^d} \sum_{\mathbf{q}} \frac{\partial_k R_k(\mathbf{q})}{\mathbf{q}^2 + R_k(\mathbf{q}) + M^2 \delta_{\mathbf{q},0} + U''_{M,k}(\phi)}. \quad (22)$$

In the limit $M = 0$, we recover the flow equation of the effective potential $U_k(m)$ (at finite size with periodic boundary conditions [56])

$$\partial_k U_k(m) = \frac{1}{2L^d} \sum_{\mathbf{q}} \frac{\partial_k R_k(\mathbf{q})}{\mathbf{q}^2 + R_k(\mathbf{q}) + U''_k(m)}, \quad (23)$$

while in the limit $M \rightarrow \infty$ the zero-momentum contribution is suppressed, and the equation for I_k reads

$$\partial_k I_k(s) = \frac{1}{2L^d} \sum_{\mathbf{q} \neq 0} \frac{\partial_k R_k(\mathbf{q})}{\mathbf{q}^2 + R_k(\mathbf{q}) + I''_k(s)}. \quad (24)$$

In the thermodynamic limit $L \rightarrow \infty$, the two sums converge to the same integral, and we recover the equivalence between the two quantities, $I_k(s) = U_k(m = s)$.

To study the critical behavior, it is convenient to introduce the dimensionless fields $\tilde{m} = k^{-(d-2)/2} m$ and $\tilde{s} = k^{-(d-2)/2} s$, and $\tilde{U}_k(\tilde{\phi}) = k^{-d} U_k(\tilde{\phi} k^{(d-2)/2})$ and $\tilde{I}_k(\tilde{\phi}) = k^{-d} I_k(\tilde{\phi} k^{(d-2)/2})$, as well as $\tilde{\mathbf{q}} = \mathbf{q}/k$. Writing the regulator as $R_k(\mathbf{q}) = k^2 \tilde{R}((\mathbf{q}/k)^2)$, the flows become

$$k \partial_k \tilde{U}_k = -d \tilde{U}_k + \frac{d-2}{2} \tilde{m} \tilde{U}'_k + \frac{1}{2(kL)^d} \sum_{\tilde{\mathbf{q}}} \frac{2\tilde{R} - \tilde{\mathbf{q}}^2 \tilde{R}'}{\tilde{\mathbf{q}}^2 + \tilde{R} + \tilde{U}_k}, \quad (25)$$

and

$$k \partial_k \tilde{I}_k = -d \tilde{I}_k + \frac{d-2}{2} \tilde{s} \tilde{I}'_k + \frac{1}{2(kL)^d} \sum_{\tilde{\mathbf{q}} \neq 0} \frac{2\tilde{R} - \tilde{\mathbf{q}}^2 \tilde{R}'}{\tilde{\mathbf{q}}^2 + \tilde{R} + \tilde{I}_k}. \quad (26)$$

In the thermodynamic limit, both flow equations become the standard dimensionless LPA equation

$$k \partial_k \tilde{U}_k = -d \tilde{U}_k + \frac{d-2}{2} \tilde{m} \tilde{U}'_k + \frac{1}{2} \int_{\tilde{\mathbf{q}}} \frac{2\tilde{R} - \tilde{\mathbf{q}}^2 \tilde{R}'}{\tilde{\mathbf{q}}^2 + \tilde{R} + \tilde{U}_k}, \quad (27)$$

and

$$k \partial_k \tilde{I}_k = -d \tilde{I}_k + \frac{d-2}{2} \tilde{s} \tilde{I}'_k + \frac{1}{2} \int_{\tilde{\mathbf{q}}} \frac{2\tilde{R} - \tilde{\mathbf{q}}^2 \tilde{R}'}{\tilde{\mathbf{q}}^2 + \tilde{R} + \tilde{I}_k}, \quad (28)$$

and at criticality, the dimensionless effective potential reaches a fixed point as $k \rightarrow 0$, that is, $\lim_{k \rightarrow 0} \lim_{L \rightarrow \infty} \tilde{U}_k = \lim_{k \rightarrow 0} \lim_{L \rightarrow \infty} \tilde{I}_k = \tilde{U}^*$, with \tilde{U}^* the solution to

$$0 = -d \tilde{U}^* + \frac{d-2}{2} \tilde{\phi} \tilde{U}^{*'} + \frac{1}{2} \int_{\tilde{\mathbf{q}}} \frac{2\tilde{R} - \tilde{\mathbf{q}}^2 \tilde{R}'}{\tilde{\mathbf{q}}^2 + \tilde{R} + \tilde{U}^{*'}}. \quad (29)$$

At large field, the last term can be neglected in Eq. (29), and \tilde{U}^* behaves as a power law:

$$\tilde{U}^* \propto \tilde{\phi}^{\frac{-2d}{d-2+\eta}}, \quad (30)$$

with $\eta = 0$ at LPA.

At finite size L and at $T = T_c$, the flow equations (25) and (26) are indistinguishable from Eqs. (27) and (28) as long as $kL \gg 1$, and \tilde{U}_k and \tilde{I}_k go to the same fixed point solution \tilde{U}^* : For $a^{-1} \gg k \gg L^{-1}$, $I_k(s) \simeq U_k(m = s) \simeq k^d \tilde{U}^*(k^{-(d-2)/2} s)$, which corresponds to the correct scaling $(d-2+\eta)/2$ with $\eta = 0$ at LPA.

However, for $kL \lesssim 1$, the flows of the $U_{M,k}$ differ significantly. In particular, the flow of the effective potential is

$$\partial_k U_k(m) \simeq \frac{1}{2L^d} \frac{\partial_k R_k(0)}{R_k(0) + U''_k(m)}, \quad (31)$$

which corresponds to the flow of a 0-dimensional theory. Because $R_k(0) \rightarrow 0$ as $k \rightarrow 0$, $U''_k(m)$ cannot stay

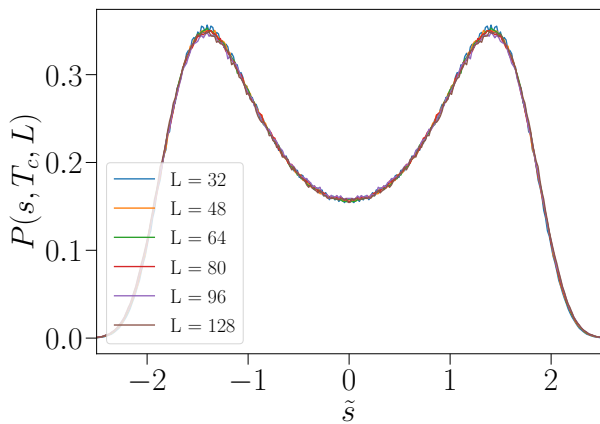


FIG. 4. Probability distribution at T_c obtained from Monte-Carlo simulations for various sizes. The finite size effects are very weak.

negative in the denominator: This induces a return to convexity, as expected for a (true) Legendre transform.

On the other hand, the flow of the rate function stops very quickly for $k \lesssim 1/L$ since the contribution of the finite momenta is negligible thanks to $\partial_k R_k(\mathbf{q})$ in this regime.

Finally, at large field ϕ , the flow of $U_{M,k}$ is barely modified by the finite size effects, and we recover the power-law behavior of the effective potential and rate function, $U_{M,k=0} \propto \phi^{\frac{2d}{d-2+\eta}}$ (with $\eta = 0$ at LPA).

III. MONTE CARLO SIMULATIONS

The PDFs were estimated numerically using Monte-Carlo simulations of the Ising model on the cubic lattice with periodic boundary conditions, using Wolff's algorithm [60]. The correlation length can be estimated using [57]

$$\xi_{\infty, \text{MC}}/a = \frac{1.073}{\sqrt{T/J}} \left(1 - \frac{T_c}{T}\right)^{-\nu}, \quad (32)$$

with $J/T_c \simeq 0.221654626$ [58] and $\nu = 0.62997$ [59]. To compute the PDF for various L and fixed ζ , the temperature is therefore chosen such that $\xi_{\infty, \text{MC}} = L/\zeta$. We performed simulations for linear sizes from $L = 16$ to $L = 128$, with for each size at least 1.5×10^7 measurements of the total spin and energy. The latter allows for using histogram reweighting [61] to explore several values of ζ in one simulation. In practice, we performed simulations for each L at $\zeta = -3, 0, 3$.

The rate function is given by

$$I(s, \xi_{\infty}, L) = \frac{-1}{L^3} \ln P(s, \xi_{\infty}, L). \quad (33)$$

At criticality, the scaling form is obtained from

$$I_{\zeta}(\tilde{s}) = L^3 I(\tilde{s}L^{-\frac{d-2+\eta}{2}}, \xi_{\infty}, L) = -\ln P(\tilde{s}L^{-\frac{d-2+\eta}{2}}, \xi_{\infty}, L). \quad (34)$$

Therefore, when expressed in terms of \tilde{s} , the probability distribution is expected to converge to a limit form, at least for sizes large enough. This happens already for moderate sizes, as finite size effects are very weak, as can be seen from Fig. 4. To obtain such a figure, for each length, the measured total spin is rescaled by $L^{\frac{d-2+\eta}{2}}$, with $\eta = 0.036298$ [59], and the data are binned into approximately 150 bins. Since the finite size effects are small, when comparing to FRG, we use the data at $L = 128$.

It is important to realize that the universality of the scaling functions $I_{\zeta}(\tilde{s})$ does not mean that all systems of the same universality class share the same rate functions, but only that they do so once the length and field normalizations have been fixed. All rate functions of a given universality class are therefore of the form $\alpha I_{\zeta}(\beta \tilde{s})$, with α and β system-dependent numbers. Therefore, the comparison between two rate functions obtained for instance in the Ising model and from FRG, is made up to two normalizations that can be chosen for instance such that they coincide at one point. We stress that α and β do not depend on ζ , and only have to be determined once.

To determine β , associated with the magnitude of the microscopic degrees of freedom, we impose that the rate function at $\zeta = 0$ has its (right) minimum at 1. For this, we locate the position of the minimum, noted \tilde{s}_0 . It is very weakly dependent on L , and we therefore use its value at $L = 128$.

The amplitude α is associated with a length scale. Note that we have chosen to shift the rate functions such that they vanish at $s = 0$. This is always feasible by changing the pre-factor of the PDF which is ultimately determined by imposing that the PDF is normalized. Therefore, it is possible to determine the amplitude α by imposing that $I_{\zeta=0}(1) = -1$. Once the two amplitudes have been determined, they are used to rescale the total spin and rate functions for all values ζ .

IV. NUMERICAL INTEGRATION OF THE LPA FLOW EQUATION

A. Numerical implementation

For the numerical integration of partial differential equations, Eqs. (23) and (24), we use the Euler method with RG time steps of 10^{-4} with $l = \ln(k/k_*)$ the RG time (integration with Runge-Kutta of order 4 gives similar results). Here k_*^{-1} is a mesoscopic length scale for which the system is self-similar, i.e. a scale much larger than the lattice spacing and at which the effective potential and rate function are described by the fixed point potential. Length scales are measured in units of k_*^{-1} .

The field dependence of functions U and I is discretized on a grid of 200 points, with the position of the minimum of the initial condition at roughly 1/4-1/5 of the grid. To integrate the flow Eqs. (23) and (24) in practice, we run

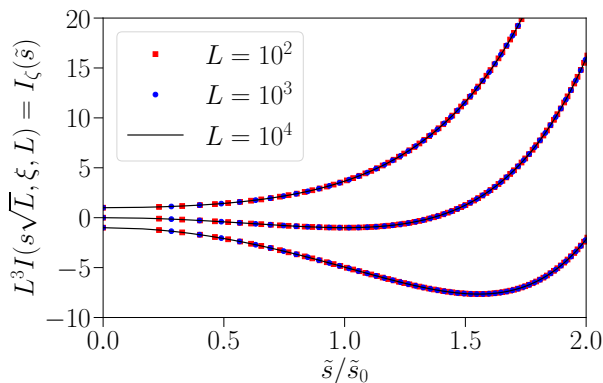


FIG. 5. Rate functions rescaled by L^d as a function of \tilde{s} at $\zeta = 3$ (top), $\zeta = 0$ (middle) and $\zeta = -3$ (bottom) obtained from FRG with the “exponential regulator” $R_k(\mathbf{q}) = \alpha k^2 e^{-\mathbf{q}^2/k^2}$ and $\alpha = 4.65$. For each value of ζ , the solid line shows the results for $L = 10^4$ in units of a mesoscopic scale k_*^{-1} at which the system becomes scale invariant. Symbols are for $L = 10^3$ (circles) and 10^2 (squares). The rate functions have been normalized as explained in the main text. This shows that the rate function obeys the expected scaling form $I(s, \xi_\infty, L) = L^{-3} I_\zeta(\tilde{s})$.

the flow in terms of dimensionless quantities, i.e. integrate Eq. (25), until $\min(kL, k\xi_\infty) \simeq 4$. Then we switch to dimensionful quantities, i.e. integrate Eq. (22), and run the flow until termination. For finite L , the sum over discrete momenta can be very demanding numerically. Therefore, we do numerical integration over the continuous variable q/k instead of sums over discrete momenta until $kL \simeq 40$. By varying all parameters of our numerical integration of the flows, we have checked that our results are converged.

B. Determination of ζ

To compare the FRG results to the MC simulations, it is necessary to compute ζ for various RG flow initial conditions. At LPA, the correlation length in the disordered phase and in the thermodynamic limit is obtained from [42]

$$\xi_{\infty, \text{FRG}}^2 = \lim_{L \rightarrow \infty} \frac{1}{U''_{k=0}(m=0)}. \quad (35)$$

In practice, we solve the flow of the effective potential of an infinite system, Eq. (27) with $M = 0$, starting from an initial condition which is the fixed point potential \tilde{U}^* perturbed by a quadratic term $\delta, \tilde{\phi}^2/2$. For $\delta = 0$, the system is critical, while it flows to the disordered (ordered) phase for $\delta > 0$ ($\delta < 0$). For small δ , the correlation length behaves as

$$\xi_{\infty, \text{FRG}} \approx \xi_+ \delta^{-\nu_{\text{LPA}}}, \quad (36)$$

with $\nu_{\text{LPA}} \simeq 0.65$, (instead of the “exact” $\nu = 0.62997$ from conformal bootstrap [59]), and ξ_+ is a non-universal

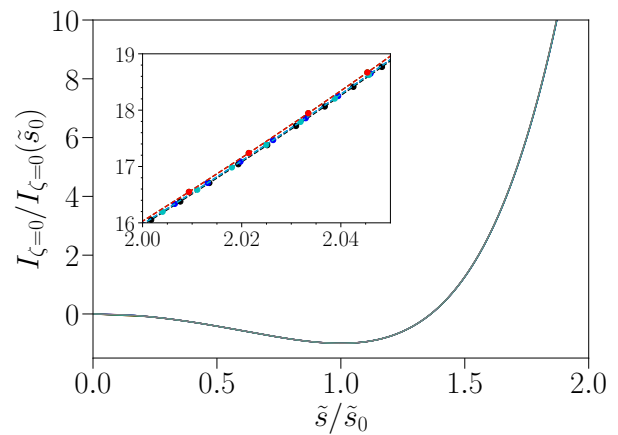


FIG. 6. Rate functions at $\zeta = 0$ obtained from FRG with the “exponential regulator” $R_k(\mathbf{q}) = \alpha k^2 e^{-\mathbf{q}^2/k^2}$ with $\alpha = 0.75$ (magenta), $\alpha = 2.5$ (black), $\alpha = 4.65$ (blue), the “Litim regulator” $R_k(\mathbf{q}) = \alpha(k^2 - \mathbf{q}^2)\theta(k^2 - \mathbf{q}^2)$ with $\alpha = 1$ (red) and $\alpha = 2$ (green), and the “Wetterich regulator” $R_k(\mathbf{q}) = \alpha \mathbf{q}^2 / (\exp(\mathbf{q}^2/k^2) - 1)$ with $\alpha = 0.75$ (gray), $\alpha = 6.05$ (cyan). The rate functions have been normalized as explained in the main text. The different results are almost indistinguishable. The inset is a zoom in the tail, showing the same data (with symbols and dashed line) and the very weak spread induced by the regulator dependence.

number. Note that ν_{LPA} and ξ_+ depend slightly on the regulator, which we take into the account to determine $\xi_{\infty, \text{FRG}}$.

To compute the rate function for a given $\zeta_{\text{FRG}} \geq 0$, at a given L , the procedure is the following. We first solve the flow of the effective potential in the thermodynamic limit, tuning δ such that the correlation length obtained from the flow is equal to L/ζ_{FRG} . Then, we compute the rate function by solving the flow (with finite L) for the same initial condition (recall that for $kL \gg 1$, the flows of I_k and U_k are identical, and that they have the same initial condition). We have checked that our results obey scaling, i.e. changing the couple (L, δ) at fixed ζ_{LPA} gives the same solution, see Fig. 5. In our comparison with MC simulations, we choose $L = 10000$. For negative ζ_{FRG} , the initial condition is the value of δ (which is negative) such that $\xi_{\infty, \text{FRG}}(-\delta) = L/|\zeta_{\text{FRG}}|$.

C. Regulator dependence

The results showed in the main text were obtained by solving the LPA equations using the “exponential regulator” $R_k(\mathbf{q}) = \alpha k^2 e^{-\mathbf{q}^2/k^2}$, where $\alpha = 4.65$ is the optimized value at LPA for this regulator (i.e. the value obtained from the Principle of Minimal Sensitivity, for which the critical exponent ν varies the least when changing α , see [53] for details). The dependence of the rate function on the regulator is very weak, as observed in Fig. 6 for $\zeta = 0$ and Fig. 7 for $\zeta = 4$.

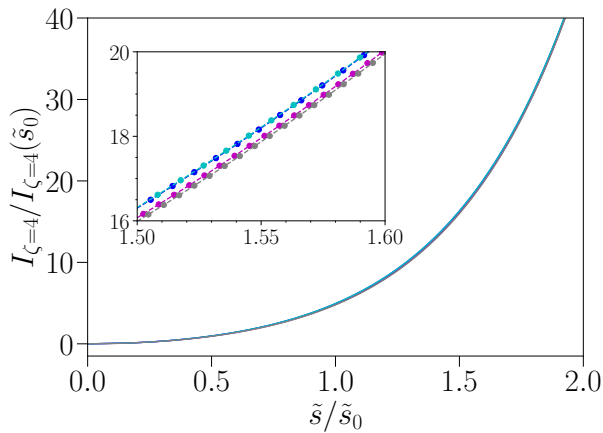


FIG. 7. Rate functions at $\zeta = 4$ obtained from FRG with the “exponential regulator” $R_k(\mathbf{q}) = \alpha k^2 e^{-\mathbf{q}^2/k^2}$ with $\alpha = 0.75$ (magenta), $\alpha = 4.65$ (blue), and the “Wetterich regulator” $R_k(\mathbf{q}) = \alpha \mathbf{q}^2 / (\exp(\mathbf{q}^2/k^2) - 1)$ with $\alpha = 0.75$ (gray), $\alpha = 6.05$ (cyan). The rate functions have been normalized using the normalization obtained for $\zeta = 0$ with the same regulator (see Fig. 6). The inset is a zoom in the tail, showing the same data (with symbols and dashed line) and the weak spread induced by the regulator dependence, see inset.

In Fig. 8, we show the regulator dependence of the fixed point effective potential. While it is expected to depend on the regulator, quite surprisingly, we observe that after normalization, the dependence is very weak. Note that this weak dependence is not an artifact of the LPA, since it can be shown in the large N limit of the $O(N)$ model, where the LPA is exact, that this dependence is still present[62].

Let us remark that the regulator functions we use in practice (see caption of Fig. 8) do not formally diverge at the beginning of the flow. This implies in practice that the initial condition of the flow is not strictly given by the mean-field approximation (i.e. $\Gamma_{M,k \sim a^{-1}}$ is not exactly given by \mathcal{H}). This is however irrelevant for the problem studied here, since we are only interested in the universal features of the PDF, which by definition are independent of the microscopic details of the model: running the flow of $\Gamma_{M,k}$ with initial conditions either given by \mathcal{H} or obtained with a finite regulator function yields the same

fixed point and scaling function $I_\zeta(\tilde{s})$.

D. Comparison with Monte-Carlo simulations

To compare our FRG calculations to the simulations, we normalize the rate functions as explained above, i.e. we impose that at $\zeta = 0$ the rate function is -1 at 1 . We use the same normalization (obtained for $\zeta = 0$) to normalize the rate function for the other values of ζ .

We have observed that if we use $\zeta_{FRG} = \zeta_{MC}$, we do not obtain a collapse of our FRG calculations with the simulations. However, allowing for a global rescaling

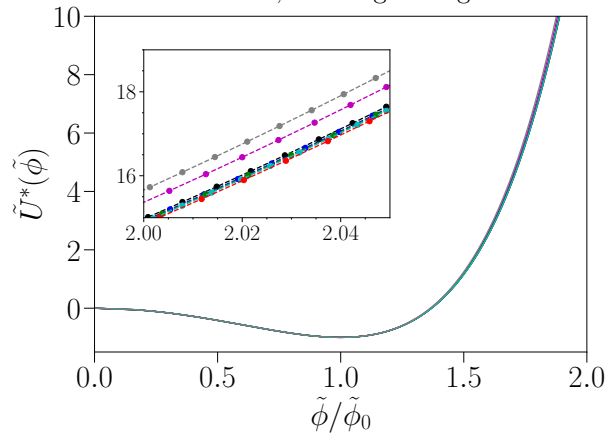


FIG. 8. Fixed point potentials obtained from FRG with the “exponential regulator” $R_k(\mathbf{q}) = \alpha k^2 e^{-\mathbf{q}^2/k^2}$ with $\alpha = 0.75$ (magenta), $\alpha = 2.5$ (black), $\alpha = 4.65$ (blue), the “Litim regulator” $R_k(\mathbf{q}) = \alpha(k^2 - \mathbf{q}^2)\theta(k^2 - \mathbf{q}^2)$ with $\alpha = 1$ (red) and $\alpha = 2$ (green), and the “Wetterich regulator” $R_k(\mathbf{q}) = \alpha \mathbf{q}^2 / (\exp(\mathbf{q}^2/k^2) - 1)$ with $\alpha = 0.75$ (gray), $\alpha = 6.05$ (cyan). They have been normalized such that $\tilde{U}^*(\tilde{\phi}_0) = -1$, with $\tilde{\phi}_0$ the position of the minimum. There is only a weak dependence on the regulator after rescaling, only showing in the tail, see inset.

$\zeta_{FRG} \simeq \zeta_{MC}/0.9$, we find a very good agreement between the two methods. We attribute that to the fact that the LPA is not exact, and that therefore the correlation length obtained from FRG is slightly off.